

Spectral and spatial coexistence of localized and extended states in disordered systems

Yi-Xin Xiao, Zhao-Qing Zhang, C. T. Chan[†]

*Department of Physics and Institute for Advanced Study, Hong Kong University of Science and Technology,
Clear Water Bay, Kowloon, Hong Kong, China*

Conventional wisdom tells us that the Anderson localized states and extended states do not coexist at the same energy. Here we propose a simple mechanism to achieve the coexistence of localized and extended states in a class of systems in which the Hilbert space can be partitioned in a way that the disorder affects only certain subspaces causing localization, while the states in the other subspaces remain extended. The coexistence of localized and extended states is achieved when the states in both types of subspaces overlap spatially and spectrally. We demonstrate such coexistence in quasi-1D and -2D disordered systems consisting of coupled diatomic chains and coupled honeycomb lattice sheets, respectively. A possible experimental realization based on coupled acoustic resonators is proposed. We show the method is very general and valid in different dimensions.

Disorder plays an important role in multiple fields of physics, such as electronics, classical waves and cold atoms^{1–4}. Anderson localization, also known as strong localization, is the absence of diffusion in disordered systems^{1,3,5}. It is a universal wave phenomenon in a disordered medium and has been extensively studied^{6–24}. Its properties depend on the disorder strength and also on the system dimension¹. It is now widely accepted that all states are localized in one- (1D) and two-dimensional (2D) disordered systems due to coherent backscattering effects^{3,25}. One remarkable feature of the Anderson localization is the existence of a mobility edge^{2,26–31} which separates the localized states from the extended states in three-dimensional (3D) random media when disorder is sufficiently strong^{1,32}. Mott argues that if a localized state and an extended

state are infinitely close in energies, they will get hybridized by an infinitesimal change of the system and turn to two extended states^{2,26}. However, a couple of exceptions were reported^{33,34}. It was shown that an inhomogeneous trap combined with a disordered potential can lead to the coexistence of localized and extended states in energy³³. The coexistence was also found in certain disordered systems with strong local symmetry³⁴.

In this work, we propose a method to create the coexistence of localized and extended states in a class of tight-binding systems. Such systems require a specific partition of the Hilbert space into subspaces so that there exists one particular subspace which does not involve all degrees of freedom of the systems. In the absence of disorder, the system is periodic and all subspaces contain bands of extended states. When disorder is introduced on the missing degrees of freedom, it only affects one subspace and makes the associated states localized, while leaving the extended states in the particular undisturbed subspace intact. The coexistence of localized and extended states is achieved by making the localized states overlap with the extended states both spectrally and spatially. Using this method, we explicitly demonstrate the coexistence of localized and extended states in both quasi-1D and quasi-2D systems with coupled diatomic chains and coupled honeycomb lattice sheets, respectively. A feasible experimental realization based on coupled acoustic resonators is proposed. Full wave computations by COMSOL show that the coexistence indeed can happen in such systems. Different from the situation in ref. 33, the coexistence in our system occurs not only in energy, but also spatially with overlapping wavefunctions. We emphasize that our method is very general. It is valid in different dimensions and can also be applied to other systems such as cold atoms and coupled optical waveguides.

Model: We first consider two identical diatomic chains³⁵ coupled indirectly through another chain as shown in Fig. 1(a). We start with a periodic system. There are five sites (“atoms”) in each unit cell, which are labeled by numbers 1 to 5. The hopping parameters between two neighboring sites are labeled as t, s, r_1 and r_2 (see Fig. 1(a)), where t and s denote respectively the intra-cell and inter-cell hoppings, while r_1 and r_2 denote the inter-chain couplings. We set the lattice constant $a = 1$ as the unit of length.

We have shown previously³⁶ that the Hilbert space of such a system can be partitioned into a topological subspace and a non-topological subspace. In the previous work, the site energies in the diatomic chains are assumed to be zero, reducing the system to two coupled SSH chains. Here the site energies in the two diatomic chains do not have to be equal, and the Hilbert space can still be partitioned as shown below.

In momentum space, the Hamiltonian has the form:

$$\mathcal{H}(k) = \begin{pmatrix} \alpha & W & 0 & 0 & r_1 \\ W^* & \lambda & 0 & 0 & 0 \\ 0 & 0 & \alpha & W & r_2 \\ 0 & 0 & W^* & \lambda & 0 \\ r_1 & 0 & r_2 & 0 & \epsilon_5 \end{pmatrix}, \quad (1)$$

where we used $W = t + se^{-ik}$ and assumed the on-site energies of sites 1 to 4 to be $\epsilon_1 = \epsilon_3 = \alpha$ and $\epsilon_2 = \epsilon_4 = \lambda$.

The partition of the Hilbert space becomes transparent if we block-diagonalize $\mathcal{H}(k)$ by using $U^{-1}\mathcal{H}(k)U = \mathcal{H}^{BD}(k)$, where

$$\mathcal{H}^{BD}(k) = \begin{pmatrix} \alpha & W & 0 & 0 & 0 \\ W^* & \lambda & 0 & 0 & 0 \\ 0 & 0 & \alpha & W & R \\ 0 & 0 & W^* & \lambda & 0 \\ 0 & 0 & R & 0 & \epsilon_5 \end{pmatrix}, \quad (2)$$

and

$$U = \frac{1}{R} \begin{pmatrix} -r_2 & 0 & r_1 & 0 & 0 \\ 0 & -r_2 & 0 & r_1 & 0 \\ r_1 & 0 & r_2 & 0 & 0 \\ 0 & r_1 & 0 & r_2 & 0 \\ 0 & 0 & 0 & 0 & R \end{pmatrix}, \quad (3)$$

where $R = \sqrt{r_1^2 + r_2^2}$. The two decoupled blocks in Eq. (2) corresponds to two separated subspaces and can be represented by two virtual lattices as shown in Fig. 1(b) and (c). Explicitly, the basis for the 2×2 block in Eq. (2) are two “hybridized orbitals”,

$$|1'\rangle = \frac{1}{R}(-r_2|1\rangle + r_1|3\rangle),$$

$$|2'\rangle = \frac{1}{R}(-r_2|2\rangle + r_1|4\rangle), \quad (4)$$

where $\langle i'|j' \rangle = \delta_{ij}$, $i, j = 1, 2$, and δ_{ij} is the Kronecker delta function.

And the basis for the 3×3 block in Eq. (2) are another three “hybridized orbitals”,

$$\begin{aligned} |3'\rangle &= \frac{1}{R}(r_1|1\rangle + r_2|3\rangle), \\ |4'\rangle &= \frac{1}{R}(r_1|2\rangle + r_2|4\rangle), \\ |5'\rangle &= |5\rangle. \end{aligned} \quad (5)$$

Since the orbital $|5\rangle$ does not appear in Eq. (4), it represents the missing degree of freedom in the subspace spanned by $|1'\rangle$ and $|2'\rangle$. As a consequence, this particular subspace will remain intact if diagonal disorder is introduced onto the 5th sites. However, the subspace relevant to the 5th sites will be affected and all states therein will become localized. We call the latter “localized” subspace and the former “extended” subspace. Since the two subspaces are orthogonal, the coexistence of localized and extended states with the same energy is possible in such a 1D disordered system. Spatially, they will also coexist since both subspaces involve sites $|1\rangle, |2\rangle, |3\rangle$ and $|4\rangle$. We want to remark that the key ingredient for the particular partition of Hilbert space is the existence of two identical diatomic chains in the system.

In the following we present a numerical demonstration for the co-existence of localized and extended states through calculations of eigenstates and the participation ratios. Numerically, we study a system of 125 unit cells. The hopping parameters are chosen to be $t = 0.7$, $s = 1.3$, $r_1 = r_2 = 1$. Without loss of generality, we assume $\alpha = \lambda = 0$ and the diatomic chain actually becomes a dimerized Su-Schrieffer-Heeger (SSH) chain³⁵. The randomness is introduced by setting the on-site energies of the 5th site within each unit cell to be a random number uniformly distributed in the range $[-2.5, 2.5]$. Consequently, the virtual lattice shown in Fig. 1(c) becomes disordered, whereas the one shown in Fig. 1(b) remain ordered. The energy spectrum is shown in Fig. 2(a), where states are classified as localized (red), extended (blue) and edge (green) states. According to the previous discussions, the localized states lie in the “localized” subspace,

whereas the extended ones lie in the “extended” subspace. The spectral overlap of two subspaces clearly demonstrates the coexistence of localized and extended states. There are three additional zero energy edge states marked by green dots, one at the left boundary and two at the right boundary. Their occurrence is due to the weak bonds at the boundaries of the two SSH chains³⁶. Actually one of the two right-boundary states stems from the disordered virtual lattice since its wavefunction conforms to Eq. (5). Another two boundary states arise from the “extended” subspace and correspond to the ordered virtual lattice. The nature of the eigenstates can be clearly characterized by the participation ratios (PR) of their wavefunctions, as shown in Fig. 2(b), where localized and extended states have sharp contrast.

To show the coexistence of two types of states, we pick two states which have almost identical energy in the overlapping region of the two subspaces and we plot their wavefunctions Ψ in Fig. 2(c), where the blue and red curves denote, respectively, the extended state at energy $E = 1.083$ and localized state at $E = 1.088$. In Fig. 2(d) we replot the wavefunctions using log scale. It shows clearly that the exponentially localized state does not couple with the extended state although they spatially overlap. The wavefunctions on each chain are also shown for the two states to reveal the subspaces they belong to. The extended state shown in Fig. 2(e) manifests anti-symmetric behavior on the two SSH chains vanishes on the middle chain; and hence it is consistent with Eq. (4) and it belongs to the “extended subspace”. Whereas for the localized state shown in Fig. 2(f), we see the wavefunction has even parity and is non-vanishing on the middle chain, which conforms to Eq. (5) and arises from the “localized” subspace.

Acoustic realization: The tight-binding model above can be easily realized by coupled acoustic cavities as shown in Fig. 3(a). The height of middle cavities takes random values in the range from 6 cm to 10 cm. The height of all other cavities is chosen to be 8 cm. The radius is chosen to be 3 cm for all cavities. Two connection tubes are used to realize the hopping t, s, r_1 or r_2 between two neighboring cavities. The lengths are 2 cm, 2cm, 1.5 cm, 1.5 cm for the tubes t, s, r_1 or r_2 , respectively. And the radii are 9 mm, 4 mm, 6 mm, 6 mm for the tubes t, s, r_1 or r_2 , respectively. We compute the eigen-system of the coupled acoustic cavities by COMSOL Multiphysics. The frequency spectrum in Fig. 3(b)

shows the overlap of the “extended” and “localized” subspaces, similar to Fig. 2(a). The wavefunctions of two neighboring states (89th and 90th) in the energy spectrum are shown in Fig. 3(c) and (d). Clearly the extended state comes from the “extended” subspace since its wavefunction has odd parity, whereas the localized state arises from the “localized” subspace due to the diagonal disorder on the middle cavities. The wavefunctions for the two neighboring states along one of the “diatomic” chains is also plotted in linear scale in Fig. 3(e) and in log scale in Fig. 3(f). The contrast between the two neighboring states is remarkable. Although the 40-cell system is not very large, we can already observe clearly Anderson localization behaviors and the coexistence of localized and extended states.

Generalization to multiple-chains: We want to emphasize that the coexistence of the localized states and extended states is not restricted to two coupled chains, it is equally valid when multiple chains are coupled. The essence is that when the diatomic chains outnumber the effective hopping channels, we are guaranteed to have a particular subspace in which there exists a set of eigenstates of the diatomic chain in the “hybridized orbitals” representation³⁶. Since the two “hybridized orbitals” in this particular subspace do not involve the coupler atoms, the disorder introduced on these coupler atoms will only localize the states in the other subspace but will not affect the extended eigenstates in this subspace. The coexistence of the localized states and extended states will occur when two subspaces overlap. We numerically investigated a finite system comprising 26 diatomic chains coupled by 25 coupler chains. There are 25 unit cells along the chain direction, amounting to a total of 1925 sites. As aforementioned, the on-site energies do not have to be equal for the realization of subspace partition. We choose two different on-site energies ($\alpha = 0.9$ and $\lambda = 1.2$) for the two non-equivalent sites on each diatomic chain. All the other sites on the coupler chains take random onsite energies ranging from 1 to 10. The intra-cell and inter-cell hoppings are chosen to be $t = 1.3$ and $s = 0.7$, respectively. All the inter-chains hoppings are chosen to be 2.5. Unlike the case in Fig. 1, there are no boundary modes in this system since the intra-cell hopping is larger than the inter-cell one. The calculated energy spectrum is shown in Fig. 4(a). An overlapping region of two subspaces is clearly seen, which implies the coexistence of two types of states. This is confirmed by the participation ratios shown in

Fig. 4(b), which unambiguously characterize the localized and extended nature for all the eigenstates. Further we show the probability distributions of two eigenstates at virtually the same energy: one localized state at $E = 1.678$ in Fig. 4(c) and the other extended state at $E = 1.679$ in Fig. (d).

Generalization to 2D (coupling two layers of honeycomb lattices): Suppose we couple two honeycomb lattice layers in the similar sense as we couple the two diatomic chains, as shown in Fig. 5(a). The same arguments used formerly to create the coexistence of localized and extended states also apply here. We computed the eigenvalues of a finite system with each honeycomb lattice layer truncated to the shape of a rectangular flake. The zigzag edges and armchair edges are along the x and y directions, respectively. The two inter-layer couplings are assumed to be $r_1 = 2$ and $r_2 = 3$, which couple only one sublattice of the two honeycomb lattice sheets. The calculated energy spectrum plotted in Fig. 5(b) shows an overlap region of localized and extended subspaces, indicating the coexistence of localized states and extended states. This is confirmed by the distinct participation ratios shown in Fig. 5(c). Apart from the extended states, there are a few edge states localized on the zigzag edges of the two honeycomb lattice layers, which are denoted by green dots. To show the coexistence, we pick two states with almost identical energies. The probability distribution $|\psi|^2$ of the extended state with energy at $E = -2.670$ is shown in (d)-(f) where (d), (e) and (f) show, respectively, the distributions in the lower, middle and upper layers. Similarly, the probability distribution $|\psi|^2$ of the localized state with energy at $E = -2.667$ is shown in (g)-(i). As expected, the wavefunction vanishes on the middle layer for the extended state, as shown in Fig. 5 (e). In contrast, the localized state has non-vanishing amplitudes on the middle layer, as shown in Fig. 5(h).

Conclusion: We propose a method to create the coexistence of localized and extended states in a class of systems where the degrees of freedoms outnumber the constraints. The coexistence is demonstrated explicitly in both quasi-1D and quasi-2D systems. We want to emphasize that the method we propose is very general. It is not limited to the coupled diatomic chains and honeycomb lattice sheets demonstrated here. It applies universally to any coupled periodic lattices as long as their identical copies outnumber the constraints

imposed by the coupler chains (layers) so that there exists a particular subspace which does not involve all degrees of freedom of the system.

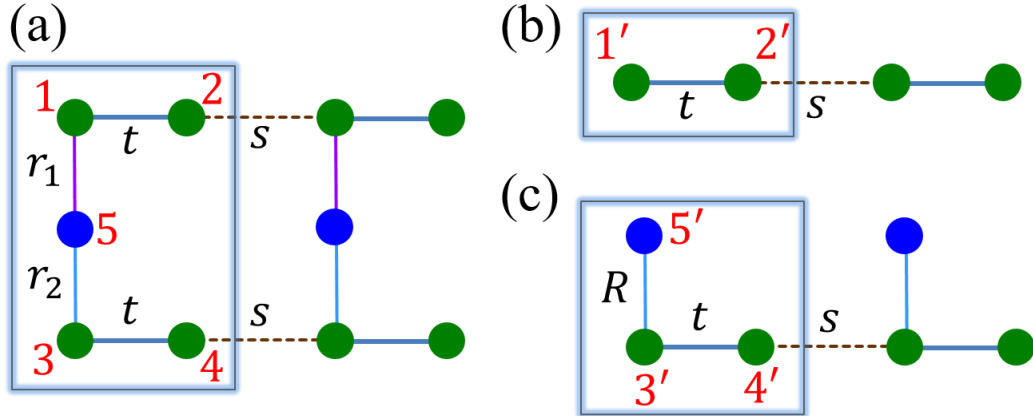
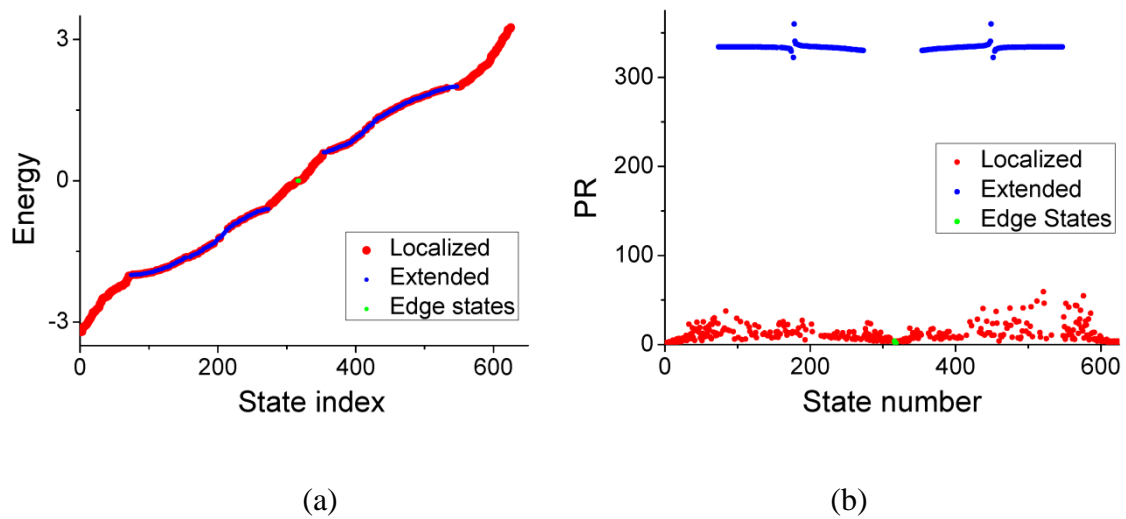


Fig. 1 (a) Two unit cells of a periodic lattice. Each cell contains five sites labeled 1 to 5. The hoppings are labeled in the 1st cell. (b) and (c) are two virtual lattices corresponding to the two partitioned subspaces of the Hilbert space of the system in (a). $R = \sqrt{r_1^2 + r_2^2}$.



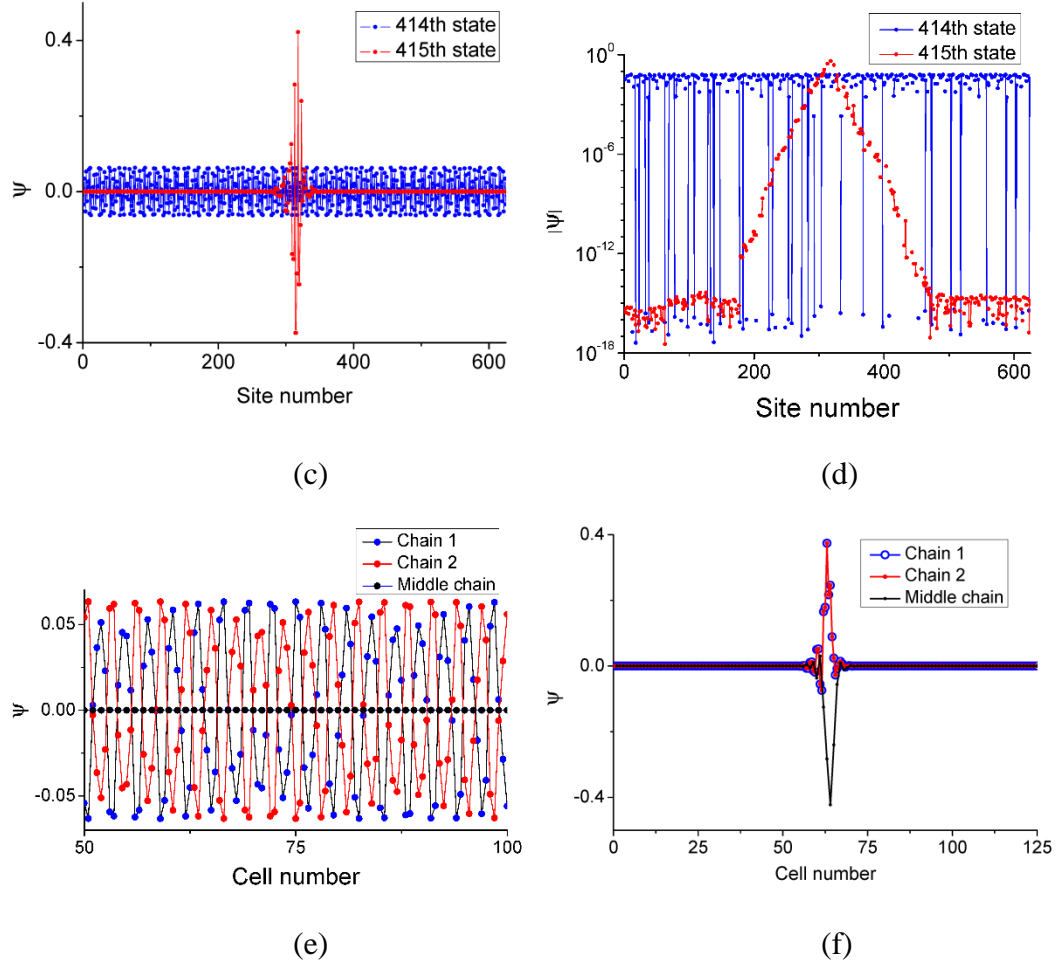
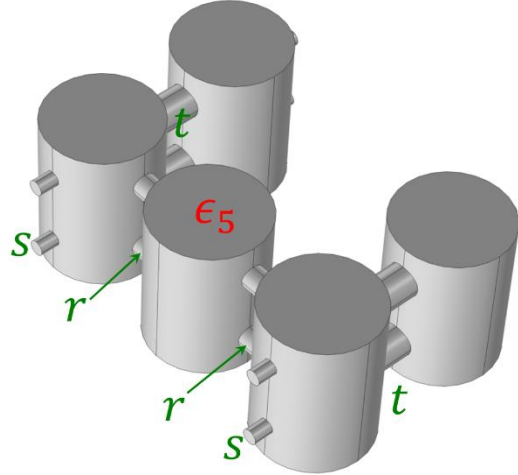
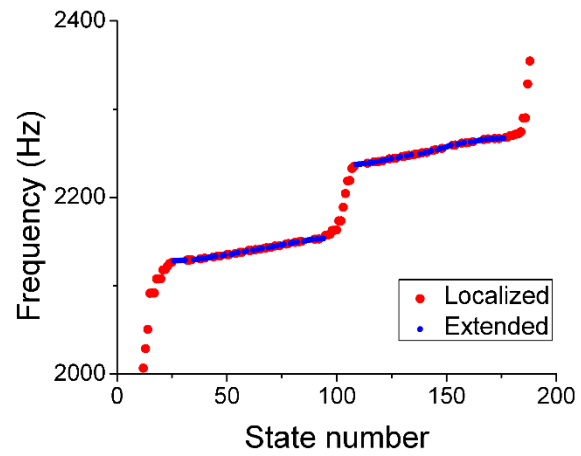


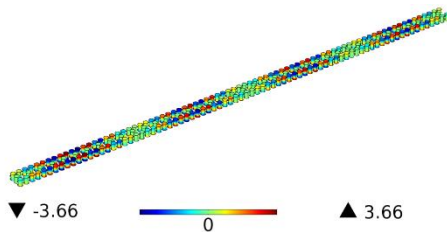
Fig. 2 (a) The energy spectrum of a 125-cell system. (b) The participation ratio of the eigenstates. (c) The wavefunctions Ψ of two eigenstates picked in the overlap region of two subspaces with almost the same eigen-energies. The horizontal axis includes all sites. (d) The log scale plot of $|\Psi|$. (e)(f) The wavefunction against the cell number on three chains for the (e) extended and (f) localized state.



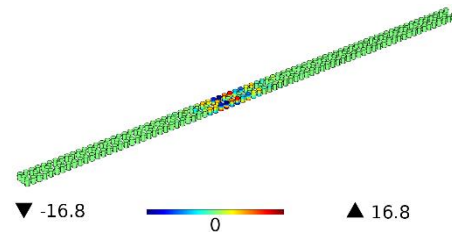
(a)



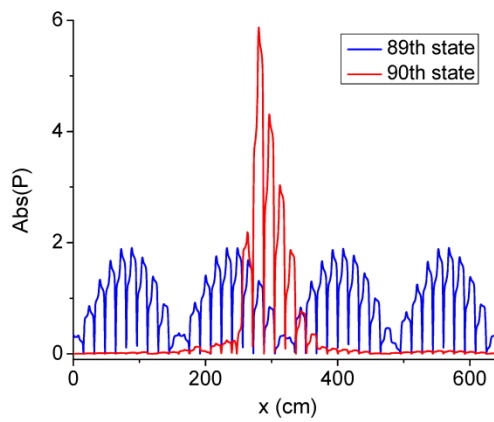
(b)



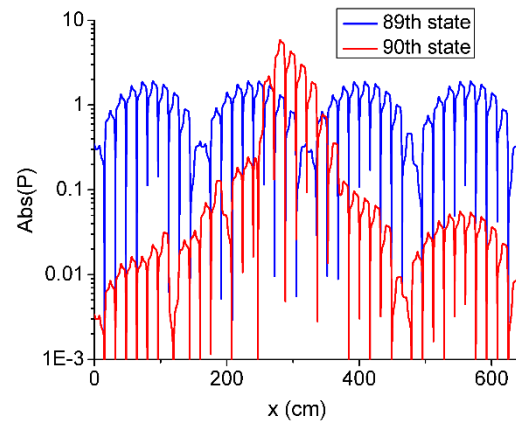
(c)



(d)



(e)



(f)

Fig. 3 (a) The unit cell of the system comprising coupled acoustic cavities for realizing the model system shown in Fig. 1(a). (b) The energy spectrum of the system. (c)(d) The pressure field distribution for the (c) 89th and (d) 90th states for a 40-cell system, where the ϵ_5 cavity in each cell takes random heights in the range from 6 cm to 10 cm. (e) The

absolute pressure field along one of the two chain for the 89th and 90th states. (f) Same as (e) but in log scale.

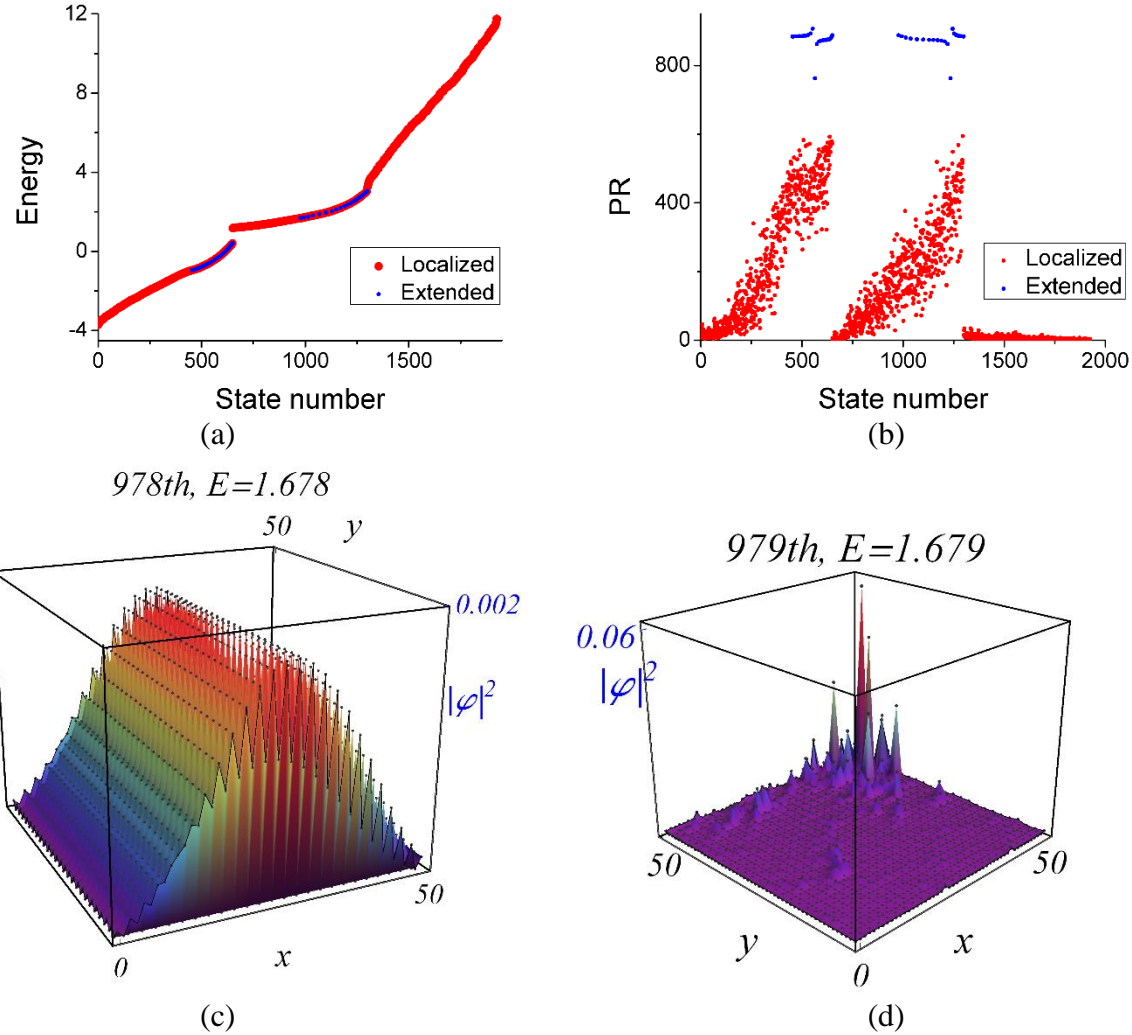


Fig. 4 (a) The energy spectrum of a finite system comprising 26 SSH chains coupled by 25 coupler chains. The system contains 25 unit cells amounting to 1925 sites. The two on-sites energies for the diatomic chains are $\alpha = 0.9$ and $\lambda = 1.2$. All the other sites on the coupler chains take random values in the range [1,10]. (b) The participation ratio of all the eigenstates. (c)(d) The probability distributions of two states at virtually the same energy: (c) extended state at 1.678 and (d) localized state at 1.679.

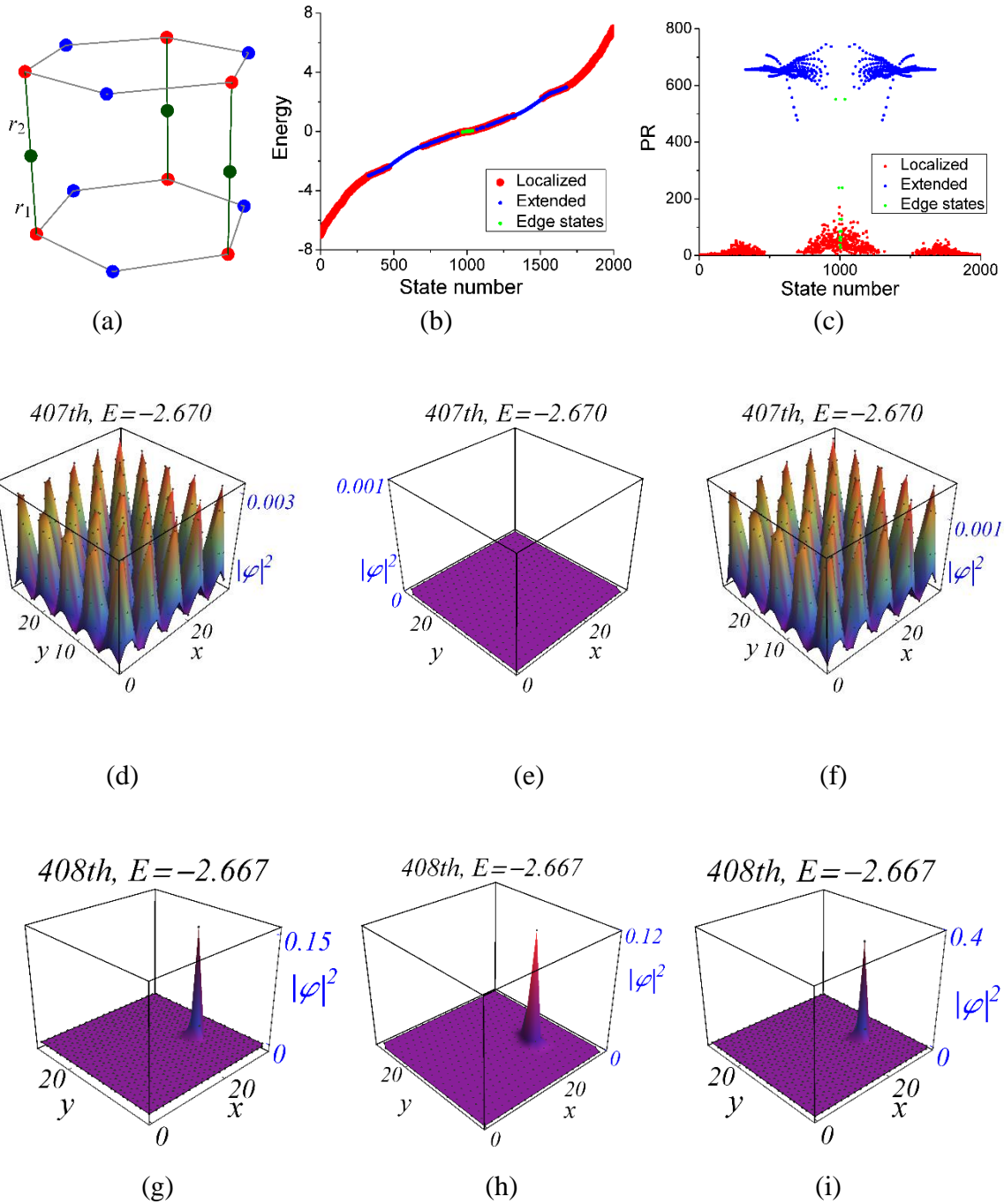


Fig. 5 (a) The unit cell for the coupled structure of two honeycomb lattice layers. (b) The energy spectrum of a finite system consisting of 400 unit cells. (c) The participation ratios of the eigenstates. (d)-(f) show the probability distributions of the 407th eigenstate on the (d) lower, (e) middle, and (f) upper layer. (g)-(i) show the probability distributions of the 408th eigenstate on the (g) lower, (h) middle, and (i) upper layer.

[†]Correspondence address: phchan@ust.hk

This work is supported by Research Grants Council Hong Kong (AoE/P-02/12).

1. Elihu Abrahams. *50 Years of Anderson Localization*. (world scientific, 2010).
2. Mott, N. F. *Metal-insulator transitions*. (Taylor & Francis, 1990).
3. Ping Sheng. *Introduction to Wave Scattering, Localization and Mesoscopic*. (Springer-Verlag Berlin Heidelberg, 2006).
4. Aspect, A. & Inguscio, M. Anderson localization of ultracold atoms. *Phys. Today* **62**, 30–35 (2009).
5. Anderson, P. W. Absence of Diffusion in Certain Random Lattices. *Phys. Rev.* **109**, 1492–1505 (1958).
6. De Raedt, H., Lagendijk, A. & de Vries, P. Transverse Localization of Light. *Phys. Rev. Lett.* **62**, 47–50 (1989).
7. Dunlap, D. H., Wu, H.-L. & Phillips, P. W. Absence of localization in a random-dimer model. *Phys. Rev. Lett.* **65**, 88–91 (1990).
8. Ye, L., Cody, G., Zhou, M., Sheng, P. & Norris, A. N. Observation of bending wave localization and quasi mobility edge in two dimensions. *Phys. Rev. Lett.* **69**, 3080–3083 (1992).
9. Wiersma, D. S., Bartolini, P., Lagendijk, A. & Righini, R. Localization of light in a disordered medium. *Nature* **390**, 671–673 (1997).
10. Chabanov, A. A., Stoytchev, M. & Genack, A. Z. Statistical signatures of photon localization. *Nature* **404**, 850–853 (2000).

11. Stärzer, M., Gross, P., Aegeerter, C. M. & Maret, G. Observation of the Critical Regime Near Anderson Localization of Light. *Phys. Rev. Lett.* **96**, 63904 (2006).
12. Topolancik, J., Ilic, B. & Vollmer, F. Experimental Observation of Strong Photon Localization in Disordered Photonic Crystal Waveguides. *Phys. Rev. Lett.* **99**, 253901 (2007).
13. Schwartz, T., Bartal, G., Fishman, S. & Segev, M. Transport and Anderson localization in disordered two-dimensional photonic lattices. *Nature* **446**, 52–55 (2007).
14. Roati, G. *et al.* Anderson localization of a non-interacting Bose–Einstein condensate. *Nature* **453**, 895–898 (2008).
15. Evers, F. & Mirlin, A. D. Anderson transitions. *Rev. Mod. Phys.* **80**, 1355–1417 (2008).
16. Lahini, Y. *et al.* Anderson Localization and Nonlinearity in One-Dimensional Disordered Photonic Lattices. *Phys. Rev. Lett.* **100**, 13906 (2008).
17. Hu, H., Strybulevych, A., Page, J. H., Skipetrov, S. E. & van Tiggelen, B. A. Localization of ultrasound in a three-dimensional elastic network. *Nat. Phys.* **4**, 945–948 (2008).
18. Chabé, J. *et al.* Experimental Observation of the Anderson Metal-Insulator Transition with Atomic Matter Waves. *Phys. Rev. Lett.* **101**, 255702 (2008).
19. Billy, J. *et al.* Direct observation of Anderson localization of matter waves in a controlled disorder. *Nature* **453**, 891–894 (2008).
20. Lahini, Y. *et al.* Observation of a Localization Transition in Quasiperiodic Photonic Lattices. *Phys. Rev. Lett.* **103**, 13901 (2009).

21. Kondov, S. S., McGehee, W. R., Zirbel, J. J. & DeMarco, B. Three-Dimensional Anderson Localization of Ultracold Matter. *Science* **334**, 66–68 (2011).
22. Jendrzejewski, F. *et al.* Three-dimensional localization of ultracold atoms in an optical disordered potential. *Nat. Phys.* **8**, 398–403 (2012).
23. Segev, M., Silberberg, Y. & Christodoulides, D. N. Anderson localization of light. *Nat. Photonics* **7**, 197–204 (2013).
24. Hsieh, P. *et al.* Photon transport enhanced by transverse Anderson localization in disordered superlattices. *Nat. Phys.* **11**, 268–274 (2015).
25. Abrahams, E., Anderson, P. W., Licciardello, D. C. & Ramakrishnan, T. V. Scaling Theory of Localization: Absence of Quantum Diffusion in Two Dimensions. *Phys. Rev. Lett.* **42**, 673–676 (1979).
26. Economou, E. N. & Cohen, M. H. Localization in disordered materials: existence of mobility edges. *Phys. Rev. Lett.* **25**, 1445 (1970).
27. Licciardello, D. C. & Thouless, D. J. Conductivity and mobility edges for two-dimensional disordered systems. *J. Phys. C Solid State Phys.* **8**, 4157 (1975).
28. John, S. Electromagnetic Absorption in a Disordered Medium near a Photon Mobility Edge. *Phys. Rev. Lett.* **53**, 2169–2172 (1984).
29. Kuhl, U., Izrailev, F. M., Krokhin, A. A. & Stöckmann, H.-J. Experimental observation of the mobility edge in a waveguide with correlated disorder. *Appl. Phys. Lett.* **77**, 633–635 (2000).
30. Delande, D. & Orso, G. Mobility Edge for Cold Atoms in Laser Speckle Potentials. *Phys. Rev. Lett.* **113**, 60601 (2014).

31. Semeghini, G. *et al.* Measurement of the mobility edge for 3D Anderson localization. *Nat. Phys.* **11**, 554–559 (2015).
32. Sheng, P. & Zhang, Z.-Q. Scalar-Wave Localization in a Two-Component Composite. *Phys. Rev. Lett.* **57**, 1879–1882 (1986).
33. Pezzé, L. & Sanchez-Palencia, L. Localized and Extended States in a Disordered Trap. *Phys. Rev. Lett.* **106**, 40601 (2011).
34. Shapir, Y., Aharony, A. & Harris, A. Localization and Quantum Percolation. *Phys. Rev. Lett.* **49**, 486–489 (1982).
35. Su, W. P., Schrieffer, J. R. & Heeger, A. J. Solitons in Polyacetylene. *Phys. Rev. Lett.* **42**, 1698–1701 (1979).
36. Xiao, Y.-X., Zhang, Z.-Q. & Chan, C. T. Coexistence of quantized and non-quantized geometric phases in quasi-one-dimensional systems without inversion symmetry. *ArXiv160500549 Cond-Mat* (2016).